

		Volume 27, issue 8, August 2012	ISSN 0883-2927
<h1>Applied Geochemistry</h1> <p>JOURNAL OF THE INTERNATIONAL ASSOCIATION OF GEOCHEMISTRY</p>			
Executive Editor Associate Editors	ROO FUGG, Aberystwyth E. L. ANDER, Nottingham L. AGULON, Rennes H. ARMANSSON, Reykjavik A. BATH, Leightonbrough G. BIRK, Gwynedd P. BIRKEL, Dübau S. BOYFILL, Leeds I. CAPWORTH, Clayton Z. CAYIROU, Ankara R. N. J. COMANS, Petten A. DANIELSSON, Linköping W. M. EDWARDS, Oxford G. FILIPPINI, Indianapolis D. FORTIN, Ottawa D. GOSLER, Wallingford	J. E. GRAY, Denver R. S. HARMON, Research Triangle Park M. HERRON, Reading M. KRISTIN, Mainz A. KRAIER, Reims X. D. LI, Guelph W. B. LYONS, Columbia H. I. MARINOVSKI, Skopje P. B. MCMURDO, Denver J. MERRILL, Jacksonville A. MUKHERJEE, Kharagpur L. A. MUNK, Anchorage B. NORDEN, Edinburgh J. C. POHL, Gif-Sur-Yvette D. PIVA, Manchester R. M. PEEK, Miami	C. REIMANN, Trondheim J. RUIZ, Linköping A. N. RYBICKI, Stellenbosch K. S. SAVAJEK, Nashville R. R. SRAJ, Il. Reims O. SUDEN, Kalmar B. R. T. SWANIGT, Corvallis D. B. SMITH, Denver S. SIBROO-GARSTON, Pinawa L. SULLIVAN, Leamoyne Y. TAYEB, Noufou A. VENGOSH, Durham P. L. VERPLANK, Denver B. WANG, Anchorage B. B. WASTY, Denver J. WEISBERG, Christchurch
<p>A. SZYNKIEWICZ, B. TALON NEWTON, S.S. TIMMONS and D.M. BORROK: The sources and budget for dissolved sulfate in a fractured carbonate aquifer, southern Sacramento Mountains, New Mexico, USA..... 1451</p> <p>Y. JIANG: Sources of sulfur in the Nandong underground river system, southwest China: A chemical and isotopic reconnaissance..... 1463</p> <p>J.M. MARQUES, P.M. CARREIRA, F. GOFF, H.G.M. EGGENKAMP and M. ANTUNES DA SILVA: Input of <sup>87</sup>Sr/<sup>86</sup>Sr ratios and Sr geochemical signatures to update knowledge on thermal and mineral waters flow paths in fractured rocks (N-Portugal)..... 1471</p> <p>S.H. WALLACE, S. SHAW, K. MORRIS, J.S. SMALL, A.J. FULLER and I.T. BURKE: Effect of groundwater pH and ionic strength on strontium sorption in aquifer sediments: Implications for <sup>90</sup>Sr mobility at contaminated nuclear sites..... 1482</p> <p>C. REIMANN, M. BERKE and P. FILZMOSER: Temperature-dependent leaching of chemical elements from mineral water bottle materials..... 1492</p> <p>K.M. CAMPBELL, R.K. KURKADAPU, N.P. QAFUKU, A.D. PEACOCK, E. LESHER, K.H. WILLIAMS, J.R. BARGAR, M.J. WILKINS, L. FIGUEROA, J. RANVILLE, J.A. DAVIS and P.E. LONG: Geochemical, mineralogical and microbiological characteristics of sediment from a naturally reduced zone in a uranium-contaminated aquifer..... 1499</p> <p>D.E. LATTI, M.I. BOYANOV, K.M. KEMNER, E.J. O'LOUGHLIN and M.M. SCHERER: Abiotic reduction of uranium by Fe(II) in soil..... 1512</p> <p>R.M. KEY, C.C. JOHNSON, M.S.A. HORSTWOOD, D.J. LAPWORTH, K.V. KNIGHTS, S.J. KEMP, M. WATTS, M. GILLESPIE, M. ADIRANMI and T. ARIBIKOLA: Investigating high zircon concentrations in the fine fraction of stream sediments draining the Pan-African Dahomeyan Terrane in Nigeria..... 1525</p> <p>A. GIELAR, E. HELIOS-RYBICKA, S. MÖLLER and J.W. EINAX: Multivariate analysis of sediment data from the upper and middle Odra River (Poland)..... 1540</p> <p>D. WAN, Z. JIN and Y. WANG: Geochemistry of eolian dust and its elemental contribution to Lake Qinghai sediment..... 1546</p> <p>Y. YU, J. SONG, X. LI and L. DUAN: Geochemical records of decadal variations in terrestrial input and recent anthropogenic eutrophication in the Changjiang Estuary and its adjacent waters..... 1556</p> <p>F. LUAN, C.M. SANTELLI, C.M. HANSEL and W.D. BURGOA: Defining manganese(II) removal processes in passive coal mine drainage treatment systems through laboratory incubation experiments..... 1567</p>			
Continued on outside back cover			

This article appeared in a journal published by Elsevier. The attached copy is furnished to the author for internal non-commercial research and education use, including for instruction at the authors institution and sharing with colleagues.

Other uses, including reproduction and distribution, or selling or licensing copies, or posting to personal, institutional or third party websites are prohibited.

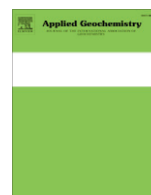
In most cases authors are permitted to post their version of the article (e.g. in Word or Tex form) to their personal website or institutional repository. Authors requiring further information regarding Elsevier's archiving and manuscript policies are encouraged to visit:

<http://www.elsevier.com/copyright>



Contents lists available at SciVerse ScienceDirect

## Applied Geochemistry

journal homepage: [www.elsevier.com/locate/apgeochem](http://www.elsevier.com/locate/apgeochem)

## Effect of groundwater pH and ionic strength on strontium sorption in aquifer sediments: Implications for $^{90}\text{Sr}$ mobility at contaminated nuclear sites

Sarah H. Wallace<sup>a</sup>, Samuel Shaw<sup>a</sup>, Katherine Morris<sup>b</sup>, Joe S. Small<sup>c</sup>, Adam J. Fuller<sup>a</sup>, Ian T. Burke<sup>a,\*</sup>

<sup>a</sup>Earth Surface Science Institute, School of Earth and Environment, University of Leeds, Leeds, West Yorkshire LS2 9JT, UK

<sup>b</sup>Research Centre for Radwaste and Decommissioning, School of Earth, Atmospheric and Environmental Sciences, University of Manchester, Manchester M13 9PL, UK

<sup>c</sup>National Nuclear Laboratory, Risley, Warrington, Cheshire WA3 6AE, UK

## ARTICLE INFO

## Article history:

Received 20 September 2011

Accepted 17 April 2012

Available online 27 April 2012

Editorial handling by A. Bath

## ABSTRACT

Strontium-90 is a beta emitting radionuclide produced during nuclear fission, and is a problem contaminant at many nuclear facilities. Transport of  $^{90}\text{Sr}$  in groundwaters is primarily controlled by sorption reactions with aquifer sediments. The extent of sorption is controlled by the geochemistry of the groundwater and sediment mineralogy. Here, batch sorption experiments were used to examine the sorption behaviour of  $^{90}\text{Sr}$  in sediment–water systems representative of the UK Sellafield nuclear site based on groundwater and contaminant fluid compositions. In experiments with low ionic strength groundwaters ( $<0.01 \text{ mol L}^{-1}$ ), pH variation is the main control on sorption. The sorption edge for  $^{90}\text{Sr}$  was observed between pH 4 and 6 with maximum sorption occurring ( $K_d \sim 10^3 \text{ L kg}^{-1}$ ) at pH 6–8. At ionic strengths above  $10 \text{ mmol L}^{-1}$ , and at pH values between 6 and 8, cation exchange processes reduced  $^{90}\text{Sr}$  uptake to the sediment. This exchange process explains the lower  $^{90}\text{Sr}$  sorption ( $K_d \sim 40 \text{ L kg}^{-1}$ ) in the presence of artificial Magnox tank liquor ( $\text{IS} = 29 \text{ mmol L}^{-1}$ ). Strontium K-edge EXAFS spectra collected from sediments incubated with  $\text{Sr}^{2+}$  in either  $\text{HCO}_3^-$ -buffered groundwater or artificial Magnox tank liquor, revealed a coordination environment of  $\sim 9$  O atoms at 2.58–2.61 Å after 10 days. This is equivalent to the  $\text{Sr}^{2+}$  hydration sphere for the aqueous ion and indicates that Sr occurs primarily in outer sphere sorption complexes. No change was observed in the Sr sorption environment with EXAFS analysis after 365 days incubation. Sequential extractions performed on sediments after 365 days also found that  $\sim 80\%$  of solid associated  $^{90}\text{Sr}$  was exchangeable with 1 M  $\text{MgCl}_2$  in all experiments. These results suggest that over long periods,  $^{90}\text{Sr}$  in contaminated sediments will remain primarily in weakly bound surface complexes. Therefore, if groundwater ionic strength increases (e.g. by saline intrusion related to sea level rise or by design during site remediation) then substantial remobilisation of  $^{90}\text{Sr}$  is to be expected.

© 2012 Elsevier Ltd. All rights reserved.

### 1. Introduction

Strontium-90 is produced in high yield (6%) during nuclear fission and is an important component of radioactive wastes. It is a pure beta emitter (half life, 28.8 a) as is its short lived  $^{90}\text{Y}$  daughter (half life, 64.2 h). If ingested  $^{90}\text{Sr}$  can substitute for Ca in human bone structure leading to irradiation of bone marrow and increased risk of diseases such as leukaemia (Pors Nielsen, 2004; O'Hara et al., 2009). Solid and liquid wastes containing high levels of fission products (e.g.  $^{90}\text{Sr}$ ,  $^{137}\text{Cs}$ ,  $^{99}\text{Tc}$ ) have been produced during nuclear reprocessing for civilian and military fuels. These wastes are often stored in large water filled tanks at or near ground surface level. Once  $^{90}\text{Sr}$  is released into the subsurface it has the potential to be highly mobile, and will remain a major contaminant for around 10 half-lives ( $\sim 300$  a). Fluids leaking from storage tanks

have led to significant levels of  $^{90}\text{Sr}$  contamination in sediments and groundwaters at a number of sites across the world, including Hanford, USA (Chorover et al., 2008; Thompson et al., 2010), Oak Ridge, USA (Saunders and Toran, 1995; Gu et al., 2005) and Mayak, Russia (Strand et al., 1999; Standring et al., 2002). Strontium-90 is also an important component of contaminant plumes originating in the separations area of the Sellafield nuclear site, UK (Gray et al., 1995), and is found in groundwater samples taken from boreholes up to 500 m from source areas (Sellafield Ltd., 2008). The predominant source of  $^{90}\text{Sr}$  at Sellafield is from tanks containing corroded MAGNOX fuel cladding (99%  $\text{Mg}(\text{OH})_2$ , pH 9–11.5), often referred to as 'Magnox sludge' (Sellafield Ltd., 2009). There are also a number of other minor plumes originating from source terms with acidic (due to  $\text{HNO}_3$ ) or circumneutral pH (Thorpe et al., 2012). At circumneutral and alkaline pH,  $\text{Sr}^{2+}$  is often readily adsorbed to sediments, potentially retarding its subsurface migration (Livens and Baxter, 1988; Choi et al., 2006). As groundwater pH at Sellafield is most commonly reported to be between pH 6 and 8 (Sellafield Ltd., 2008),  $^{90}\text{Sr}$  migration has been assumed to

\* Corresponding author.

E-mail address: [i.burke@see.leeds.ac.uk](mailto:i.burke@see.leeds.ac.uk) (I.T. Burke).

be controlled by sorption reactions (Sellafield Ltd., 2008), including adsorption onto clay minerals such as illite, chlorite, kaolinite or montmorillonite present in the sediments (Trivedi and Axe, 1999; Dyer et al., 2000).

In general,  $\text{Sr}^{2+}$  adsorbs to a wide range of aluminosilicates, Fe oxides and other soil minerals via weakly bound outer-sphere surface complexes at the solid water interface (Patterson and Spoel, 1981; Torstenfelt et al., 1982; Higgo, 1987; Saunders and Toran, 1995; Parkman et al., 1998; O'Day et al., 2000; Sahai et al., 2000; Chorover et al., 2008). The degree of  $^{90}\text{Sr}$  adsorption depends on a number of factors, such as pH, ionic strength, composition of the solid phase and surface area (Higgo, 1987). Batch sorption studies have reported that Sr adsorption to minerals such as illite (Bilgin et al., 2001), montmorillonite (Lu and Mason, 2001), kaolinite (Bascetin and Atun, 2006) and hydrous ferric oxide (HFO) (Small et al., 1999) occurs rapidly (in 1–24 h) at pH values between 3 and 13. The affinity of Sr for swelling clays such as montmorillonite is reported to be greater than for non-swelling clays such as kaolinite (Bascetin and Atun, 2006). This was attributed to the expanding properties of montmorillonite which allow  $\text{Sr}^{2+}$  ions to penetrate between the silicate layers, whereas kaolinite can absorb  $\text{Sr}^{2+}$  to the outer surface only. Sorption of  $\text{Sr}^{2+}$  to clay minerals and Fe oxyhydroxides as a function of pH follows standard models for outer sphere cation adsorption to amphoteric mineral surfaces (Krauskopf and Bird, 1995). At low pH (below the point of zero charge (PZC) for the mineral) low levels of adsorption occur, with higher levels of adsorption at higher pH above the PZC (Sposito, 1989). The pH of the Sr-sorption edge for a particular soil/sediment is, therefore, highly dependent on the PZC of the adsorbing minerals present. Due to the predominance of outer sphere bonding, the extent of  $\text{Sr}^{2+}$  sorption on natural materials is reduced by the presence of competing divalent cations with smaller ionic radius, such as aqueous  $\text{Ca}^{2+}$  and  $\text{Mg}^{2+}$  (Marinin and Brown, 2000). Adsorption of  $\text{Sr}^{2+}$  is reported to be less affected by the presence of monovalent cations such as  $\text{Na}^+$  and  $\text{K}^+$  (Hull and Schafer, 2008). This is relevant to nuclear legacy sites, where the ionic strength of contaminant plumes is often high (Zachara et al., 2004).

At longer equilibration times (days to years), intra-particle diffusion, mineral dissolution/recrystallisation and particle ripening can lead to the incorporation of  $\text{Sr}^{2+}$  into newly formed mineral phases (Chorover et al., 2008). For example,  $\text{Sr}^{2+}$  can readily substitute into  $\text{Ca}^{2+}$  sites during carbonate precipitation (Parkman et al., 1998) and can form insoluble strontianite ( $\text{SrCO}_3$ ) surface precipitates at high pH (Liu et al., 1991; Sahai et al., 2000). Also, in experiments where Sr adsorbed to Fe oxides or sediments were aged in the presence of atmospheric  $\text{CO}_2$ , a Sr-carbonate like coordination environment was observed in EXAFS spectra (Sahai et al., 2000; Chorover et al., 2008); consistent with the formation of Sr-bearing carbonate mineral phases.

Here, results are presented from a series of batch sorption experiments designed to investigate the behaviour of  $^{90}\text{Sr}$  in sediments, representative of the UK Sellafield site. The specific objective of the study was to investigate the effect of several relevant groundwater compositions on  $\text{Sr}^{2+}$  sorption and mobility. The effect of variation in pH (from pH 2 to 10) and cation competition from monovalent ( $\text{Na}^+$ ) and divalent ( $\text{Ca}^{2+}$ ) cations on Sr sorption was also determined. A Langmuir isotherm for Sr-sorption, providing an estimate of the maximum binding capacity of Sr onto Sellafield representative sediments, has been determined in circumneutral pH and Magnox leachate affected sediment-water systems. To assess potential long-term changes in  $^{90}\text{Sr}$  sorption behaviour, selected experiments were performed over one year, and a combination of sequential extraction and X-ray absorption spectroscopy was used to determine solid phase Sr speciation.

## 2. Materials and methods

### 2.1. Sediment collection

Samples representative of the glacial/fluvial unconsolidated quaternary deposits that underlie the UK Sellafield nuclear site (McMillan et al., 2000; Law et al., 2010) were collected in August 2009 from the River Calder valley, Cumbria, UK (Lat 54°26.3'N, Long 3°28.2'W) (Fig. 1). Sediment was stored in HDPE plastic containers, dried at 40 °C and sieved to retain the less than 2 mm fraction prior to use.

### 2.2. Sediment characterisation

Powder X-ray Diffraction (XRD) analysis was performed on the bulk sediment and a separated fine particle size fraction. The fine fraction separation was produced by preparing 500 mL of a 50 g L<sup>-1</sup> sediment suspension with 0.375 g L<sup>-1</sup> sodium silicate solution (Schramm and Scripture, 1925). The mixture was stirred for 1 h, left for 24 h, and stirred again for 1 h. After a further 7 days settling the top 200 mL of supernatant was removed. The suspension was dried for 24 h at 50 °C to remove excess water. The dry sample was then washed three times in methanol (Whittig and Allardice, 1986) prior to final drying and analysis. Diffraction patterns were collected from the bulk sediment sample from 5° to 70° 2 $\theta$ , step size of 0.01 and 0.5 s/step, using a Philips PW1770 X-ray diffractometer with a Cu tube ( $\lambda = 1.54056 \text{ \AA}$ ). The fine fraction sample was analysed for 23 h from 5° to 90° on a Bruker D8 Advance XRD with a Cu tube.

Sediment was prepared for scanning electron microscopy (SEM) analysis as follows: Approximately 5 g sediment was vacuum embedded in epoxy resin and polished with grinding paste in water suspension. The polished resin block was carbon coated prior to analysis on a CamScan Series 4 SEM using backscattered electron imaging at 20 kV and a working distance of 31 mm. Energy dispersive X-ray microanalysis (EDX) was performed on selected ~10  $\mu\text{m}$  spots using an Oxford Instruments INCA 250 system. Grainsize distribution was determined by sieving 10 g sediment three times using standard laboratory sieves. Sediment pH was determined from a 1 g:1 mL suspension of sediment in deionised water using a pH electrode (ASTM, 2006). Exchangeable Sr in the sediment was determined by extraction (1 g per 10 mL) with a 1 mol L<sup>-1</sup>  $\text{MgCl}_2$  solution, followed by determination of Sr concentration in the extract on a Perkin Elmer 5300DV ICP-OES. Sediment

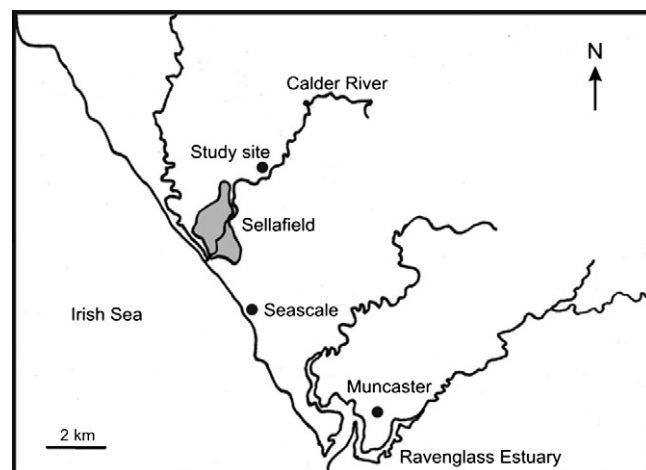


Fig. 1. Location of the sediment sampling location with respect to the UK Sellafield nuclear site (shaded in grey).

cation exchange capacity (CEC) was determined based on sorption of 0.01 M Cu(II) triethylenetetramine followed by spectrophotometric determination of the coloured solution at 577 nm on a Jenway 6715 UV/Visible spectrophotometer (Honty et al., 2010).

### 2.3. Batch sorption experiments

Dried sediment was reacted with four different groundwater solutions in 100 mL HDPE Erlenmeyer flasks using a solid:solution ratio of 100 g L<sup>-1</sup> (see Table 1). This ratio is lower than those typically found under field conditions (~1000 g L<sup>-1</sup>; Limousin et al., 2007), and was chosen so that experimental  $K_d$  values could be easily determined from the activity of <sup>90</sup>Sr measured in solution. All experiments were performed in triplicate in the dark at room temperature. To limit CO<sub>2</sub> dissolution the artificial Magnox tank liquor (pH 11) was prepared in an anaerobic chamber (97% N<sub>2</sub>: 3% H<sub>2</sub>; Coy Ltd., CA) and experiments were carried out in sealed flasks with Ar headspace maintained throughout sampling and analysis. Experiments at lower pH (<8) were carried out with an air headspace with no control on CO<sub>2</sub> ingress. At these pH values and solution compositions, oversaturation with respect to carbonate phases was not predicted using PHREEQC modelling. All sediments were left to equilibrate with groundwaters for 24 h then spiked with <sup>90</sup>Sr tracer (as SrCl<sub>2</sub> in 0.01 M HCl; CERCA-LEA, France) to a final specific activity of 30 Bq mL<sup>-1</sup> ( $5.9 \times 10^{-9}$  mol L<sup>-1</sup>). Using radioactive <sup>90</sup>Sr tracer allowed experiments to be carried out at environmentally relevant concentrations, similar to those found in Sellafield contaminated land (Sellafield Ltd., 2008). After spiking, each flask was agitated on an orbital shaker at 125 rpm. Samples were withdrawn at 1, 4, 24 and 48 h after <sup>90</sup>Sr addition. At each sampling point, 1.2 mL was removed from each flask and centrifuged at 16,000g for 10 min, then 1 mL of the supernatant was removed to determine total <sup>90</sup>Sr + <sup>90</sup>Y activity by liquid scintillation counting (1 mL sample per 10 mL EcocintA, National Diagnostics USA; count time, 10 min; energy window, 30–1020 keV) on a Packard Tri-Carb 2100TR Liquid Scintillation Analyzer. Samples were decay stored for a minimum of 35 days prior to counting to allow for secular equilibrium with <sup>90</sup>Y to be attained, and for any unsupported aqueous <sup>90</sup>Y present to decay below detection limits. Experimental pH was also determined on an Orion bench top meter (using electrodes calibrated at pH 4, 7 and 10) before and after sediment addition and at the 48 h time point. In all tests the % <sup>90</sup>Sr sorption was calculated from activities of <sup>90</sup>Sr in solution as follows:

$$\% \text{ } ^{90}\text{Sr}_{\text{sorb}} = \frac{A_i - A_e}{A_i} \times 100 \quad (1)$$

**Table 1**  
Composition of artificial groundwater solutions used in experiments.

Groundwater solution	Composition (g L <sup>-1</sup> )/ production method
A Nitric acid effected GW	As Solution B adjusted to pH 3.5 with HNO <sub>3</sub>
B Unbuffered GW <sup>a</sup>	0.0066 g KCl, 0.0976 g MgSO <sub>4</sub> ·7H <sub>2</sub> O, 0.0810 g MgCl <sub>2</sub> ·6H <sub>2</sub> O, 0.0829 g Na <sub>2</sub> SiO <sub>3</sub> , 0.0275 g NaNO <sub>3</sub> , 0.0094 g NaCl added to 1 L DIW. SrCl <sub>2</sub> solution was added to achieve a final Sr <sup>2+</sup> concentration of 1 mg L <sup>-1</sup> ( $1.14 \times 10^{-5}$ mol L <sup>-1</sup> )
C Bicarbonate buffered GW	As Solution B with 0.2424 g NaHCO <sub>3</sub>
D Magnox tank liquor <sup>b</sup>	0.38 g NaNO <sub>3</sub> , 0.1 g Mg(NO <sub>3</sub> ) <sub>2</sub> ·6H <sub>2</sub> O, 0.47 g KNO <sub>3</sub> , 0.21 g Na <sub>2</sub> CO <sub>3</sub> , 0.04 g CaCl <sub>2</sub> ·2H <sub>2</sub> O, 0.07 g Al <sub>2</sub> (NO <sub>3</sub> ) <sub>3</sub> ·6H <sub>2</sub> O, 0.023 g Na <sub>2</sub> SO <sub>4</sub> in 1 L DIW deoxygenated with N <sub>2</sub> and adjusted to pH 11 by addition of 1.2 mL 10 M NaOH

<sup>a</sup> Based on composition given in Wilkins et al. (2007).

<sup>b</sup> Based on generic tank fluid composition (Sellafield Ltd., 2009).

where  $A_i$  is the initial added activity (Bq mL<sup>-1</sup>),  $A_e$  is the activity after sorption (Bq mL<sup>-1</sup>).

Further, the apparent distribution coefficient between solid and aqueous phase ( $K_d$ , L kg<sup>-1</sup>) was calculated using the following equation (Khan et al., 1995):

$$K_d = \frac{A_i - A_e}{A_e} \times \frac{V}{W} \quad (2)$$

where  $V$  is the solution volume (mL) and  $W$  is the weight of sediment (g).

The effect of pH variation was determined in additional sorption tests performed in triplicate, with solid solution ratio of 100 g L<sup>-1</sup>, and using the artificial unbuffered groundwater solution (Table 1, Solution B) as the background electrolyte. A pH titration over a pH range of 2–10 was achieved in replicate experiments by addition of progressively more concentrated HCl or NaOH solutions. Similarly the effect of Ca<sup>2+</sup> and Na<sup>+</sup> competition was investigated in the HCO<sub>3</sub><sup>-</sup> buffered groundwater solution (pH 7.2) by addition progressively more concentrated CaCl<sub>2</sub> and NaCl solutions ( $0.1 \times 10^{-4}$ – $0.1$  mol L<sup>-1</sup>). The solutions and sediments were mixed for 24 h prior to spiking with <sup>90</sup>Sr tracer, after which they were agitated for 48 h at 125 rpm, before pH and <sup>90</sup>Sr activity was determined as above.

Sorption isotherm experiments were carried out for HCO<sub>3</sub><sup>-</sup> buffered groundwater (pH 7.2), and simulated Magnox tank liquor (pH 11). Experiments were carried out in 40 mL Oak Ridge tubes at a solid:solution ratio of 40 g L<sup>-1</sup>, using SrCl<sub>2</sub> as a source of Sr<sup>2+</sup> ions in incremental concentrations from  $5 \times 10^{-5}$  mol L<sup>-1</sup> to  $1 \times 10^{-1}$  mol L<sup>-1</sup>. Experiments for each concentration were carried out in triplicate. Again, the solutions and sediments were mixed for 24 h prior to pH measurement and spiking with <sup>90</sup>Sr tracer to a final specific activity of 30 Bq mL<sup>-1</sup>. All tubes were agitated horizontally on an orbital shaker at 75 rpm for 48 h. After 48 h, final solution pH was measured before the tubes were centrifuged at 6000g for 10 min and the supernatant analysed for <sup>90</sup>Sr activity as above.

Experimental data were fitted to the Langmuir sorption equation shown below using computer software (LMMpro version 1.06, Alfisol Ltd.) to calculate  $S_{\text{max}}$  (the maximum sorption capacity)  $K_{\text{ads}}$  (the apparent Langmuir adsorption constant) and  $R_2$  (goodness of fit in vertical non-linear least squares regression).

$$[\text{Sr}_{\text{sorb}}] = \frac{S_{\text{max}} K_{\text{ads}} [\text{Sr}_{\text{sol}}]}{1 + K_{\text{ads}} [\text{Sr}_{\text{sol}}]} \quad (3)$$

### 2.4. Sorption modelling

Data obtained from batch experiments examining the effect of Ca<sup>2+</sup> and Na<sup>+</sup> competition on Sr<sup>2+</sup> ion exchange were interpreted with the aid of the PHREEQC geochemical speciation program (Parkhurst and Appelo, 1999). Speciation calculations were performed with the wateq4f.dat thermodynamic database distributed with PHREEQC, which includes generic ion exchange constants for Ca<sup>2+</sup>, Na<sup>+</sup>, K<sup>+</sup>, Mg<sup>2+</sup> and Sr<sup>2+</sup> (Appelo and Postma, 2005) that were empirically altered to improve model fits to experimental data. Modelling calculations simulated the addition of CaCl<sub>2</sub> and NaCl<sub>2</sub> to the carbonated buffered groundwater in contact with an ion exchange concentration of  $8.2 \times 10^{-3}$  mol L<sup>-1</sup> of solution equivalent to the measured CEC. The exchange constants were varied and the exchanger concentration increased to  $3 \times 10^{-2}$  mol L<sup>-1</sup> of solution to aid the interpretation by assessing how well the Sr<sup>2+</sup> sorption could be explained by the ion exchange model. The effect of surface complexation of Sr<sup>2+</sup> on Fe oxides (Dzombak and Morel, 1990) was also considered using the Fe-oxide concentration determined by (Law et al., 2010), but was found to make a negligible contribution

to overall sorption in the HCO<sub>3</sub>-buffered groundwater solution at pH 7.2.

### 2.5. Long-term Sr sorption experiments

Long-term sorption experiments were carried out for the HCO<sub>3</sub>-buffered groundwater and Magnox liquor compositions. Dried sediment was weighed into Oak Ridge tubes and mixed with the buffered groundwater/Magnox solutions containing 20 mg L<sup>-1</sup> Sr<sup>2+</sup> at a solid:solution ratio of 20 g L<sup>-1</sup>, in an anaerobic chamber. A lower solid:solution ratio and elevated Sr<sup>2+</sup> concentration was used in these experiments so that the final solid phase Sr concentration was ~500–1000 mg Kg<sup>-1</sup>. This was the lowest concentration where useful Sr K-edge EXAFS data could be acquired. All tubes were stored inside airtight jars containing Carbosorb™, in the dark, for up to a year. Triplicate tubes were sacrificially sampled at 10, 30, 90 and 365 days. In addition, a replicate set of three tubes for each time point were spiked with 30 Bq mL<sup>-1</sup> <sup>90</sup>Sr tracer under Ar, for sequential extractions. At each sampling point, non-active tubes were centrifuged at 6000g for 10 min, the supernatant removed and the moist sediment stored at -80 °C prior to X-ray absorption spectroscopy (XAS) analysis.

Sequential extractions were carried out on tubes containing <sup>90</sup>Sr at each time point following an adapted Tessier/BCR method (Tessier et al., 1979; Burke et al., 2010). The tubes were spun at 6000g for 10 min, and the porewater removed and filtered (0.2 μm). The sediment was then progressively leached with 1 mol L<sup>-1</sup> MgCl<sub>2</sub> (pH 7, 2 h, exchangeable fraction), 1 mol L<sup>-1</sup> sodium acetate (pH 5, 5 h, carbonate fraction) and finally 0.5 mol L<sup>-1</sup> hydroxylammonium chloride (pH 1.5, 12 h, reducible fraction). Between each stage the tubes were centrifuged and the supernatant removed and filtered as before. A 1 mL sample of each extraction leachate was analysed for <sup>90</sup>Sr content by LSC as described above.

### 2.6. X-ray absorption spectroscopy

Strontium K-edge (14,165 eV) spectra were collected in January 2011 at the Dutch-Belgian beamline BM26A at the European Synchrotron Radiation Facility (ESRF) operating at 6 GeV with a typical current of 190 mA, using a N<sub>2</sub> cooled Si(1 1 1) double crystal monochromator and focussing optics. A pair of collimating mirrors was used to reduce the harmonic content of the beam and the beam size was approximately 0.1 × 3 mm at the sample (see Nikitenko et al., 2008, for further details of station step-up and protocols). Spectra were collected from sediment samples aged in both groundwater and Magnox liquor based solutions at sample points of 10 or 365 days. For analysis, approximately 300 mg moist sediment samples were prepared under an Ar atmosphere by packing in Al or Teflon holders with Kapton™ tape windows. All sediment samples were transported to the ESRF at -78 °C using dry ice. All data were collected in fluorescence mode using a nine element solid state Ge detector. Sediment sample data were collected at 80 K using an Oxford Instruments CCC 1204 liquid N<sub>2</sub> cooled cryostat. Results were compared to data collected from an aqueous Sr<sup>2+</sup> standard (3000 mg L<sup>-1</sup> as SrCl<sub>2</sub>) collected at room temperature, also held in a Teflon holder using Kapton™ tape windows. Multiple scans were averaged to improve the signal to noise ratio using Athena version 0.8.061 (Ravel and Newville, 2005) and data were background subtracted for EXAFS analysis using PySpline v1.1 (Tenderholt et al., 2007).

EXAFS data were analysed in DLExcurv v1.0 (Tomic et al., 2005) using full curved wave theory (Gurman et al., 1984). Phaseshifts were derived from *ab initio* calculations using Hedin–Lundqvist potentials and von-Barth ground states (Binsted, 1998). Fourier transforms of the EXAFS spectra were used to obtain an approximate radial distribution function around the central Sr atom (the

absorber atom); the peaks of the Fourier transform can be related to “shells” of surrounding backscattering ions characterised by atom type, number of atoms, absorber–scatterer distance, and the Debye–Waller factor ( $\pm 25\%$ ),  $2\sigma^2$ . Atomic distances calculated by DLExcurv have an error of approximately  $\pm 0.02$  Å in the first shell. The data were fitted for each sample by defining a theoretical model and comparing the calculated EXAFS spectrum with experimental data. Shells of backscatterers were added around the Sr atom and by refining an energy correction Ef (the Fermi Energy; which for final fits typically varied between -3.8 and -2.6), the absorber–scatterer distance, and the Debye–Waller factor for each shell, a least squares residual (the R factor; Binsted et al., 1993) was minimised. The amplitude factor (or AFAC in DLExcurv V1.0) was retained as the default of 1 throughout. Shells or groups of shells were only included if the overall fit (R-factor) was reduced overall by >5%. For shells of backscatterers around the central Sr, the number of atoms in the shell was chosen as an integer to give the best fit and then further refined.

## 3. Results

### 3.1. Sediment characterisation

Sediment from the same location has been described previously (Law et al., 2010). Briefly, XRD analysis showed that it was composed of quartz, muscovite, chlorite, albite and microcline. In addition, the extracted fine particle fraction was dominated by chlorite, but also contained minor amounts of illite, hematite, goethite and microcline. This suggests that clay phases are present within the sediment, but are undetectable in the bulk sample probably due to the low proportion present (<1%) and the low crystallinity of these phases. Air dried soil was reddish-brown in colour and was assigned a Munsell colour notation of 2.5YR 4/8. The sediment can be described as an angular, poorly sorted sandy loam (approximate particle composition of 53% sand, 42% silt, 5% clay), consistent with glacial weathering and deposition. Sediment pH was ~5.4. The major elemental composition was Si (35.0%), Al (5.81%), Fe (3.09%) and K (2.68%). Natural Sr was present as a minor element at 58 ppm. Exchangeable Sr was not detected in MgCl<sub>2</sub> extractions; therefore, all of the natural Sr in the sediment must be ascribed to mineral matrices. The concentration of weak acid extractable Fe(III) in the sediment was  $8.2 \pm 0.9$  μmol g<sup>-1</sup> and the organic matter content was  $0.56 \pm 0.08$  wt% (Law et al., 2010). The cation exchange capacity was determined as  $8.2 \pm 5.1$  meq 100 g<sup>-1</sup> and the BET surface area was  $3.4 \pm 0.6$  m<sup>2</sup> g<sup>-1</sup>. Backscatter electron imaging photomicrographs of resin embedded Sellafield sediment showed the sediment was composed of mostly angular grains 50–600 μm in size (Fig. 2). Energy dispersive X-ray analysis from spots (~10 μm) within the larger grains was consistent with the composition of quartz (Si and O only) or feldspar (Si, Al, O, and K/Na) (data not shown) consistent with a rock fragment derived sediment. The larger grains were commonly found to be coated with a 10–50 μm rinds of fine grained material (Fig. 2b) which contained Si, Al, K and Fe (Fig. 2c and d). This is consistent with the presence of a mixed assemblage of aluminosilicate clays and Fe oxide minerals.

### 3.2. Synthetic groundwater and pH 2–10 adsorption behaviour

Strontium-90 uptake to the sediment was rapid in all experimental groundwaters with the majority of <sup>90</sup>Sr sorption occurring within 4 h. After this time there was only a small increase in <sup>90</sup>Sr sorption measured at 24 h and 48 h in all systems (Fig. 3). The range of pH, % <sup>90</sup>Sr sorption and *K<sub>d</sub>* determined after 48 h for each synthetic GW system are shown in Table 2. There was a small change of less than 0.5 pH units between the initial solution pH and the

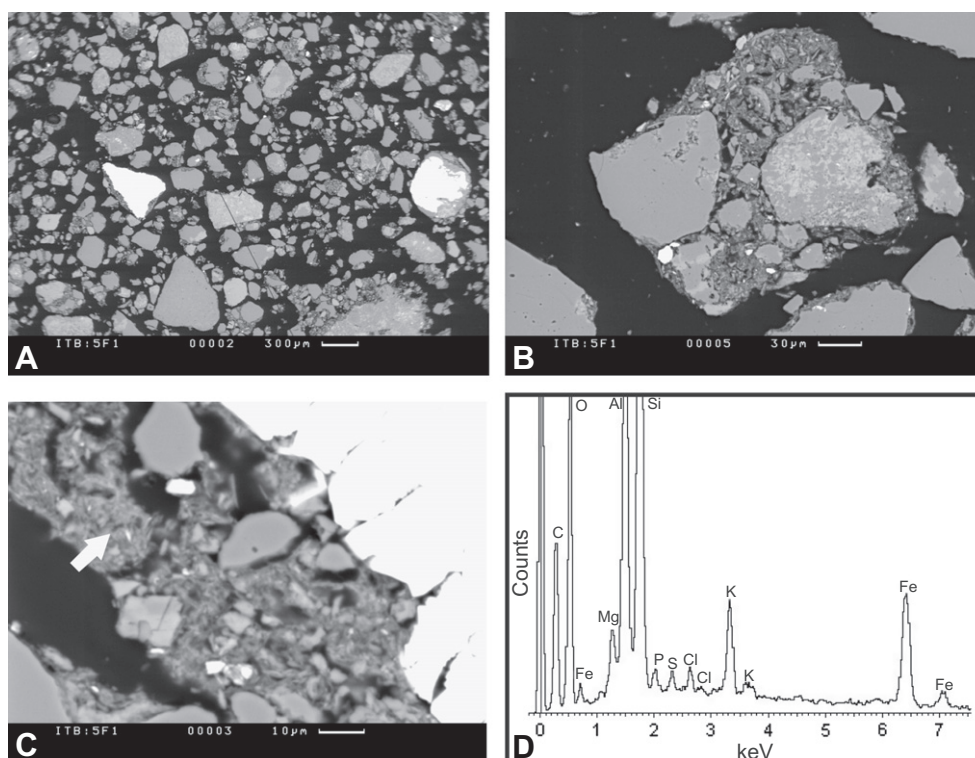


**Fig. 2.** Backscatter electron imaging photomicrographs of Sellafield sediment showing; (a) low resolution image of range of sediment grains (scale bar = 300 μm) suspended in polished epoxy resin block; (b) image of single aggregate several grains and fine grained particle coating (scale bar = 30 μm); (c) high resolution image of fine grained particle coating material (scale bar = 10 μm); (d) energy dispersive X-ray analysis spectrum of fine material taken from point shown in (c) with white arrow. (The Cl peaks are due to the resin used to embed the sample.)

pH determined after 48 h in contact with sediments in groundwater systems. However the artificial Magnox tank liquor system showed a significant pH reduction from pH 11 to around pH 7.8 at 48 h, indicating that rapid buffering by the sediment had occurred. Sorption of  $^{90}\text{Sr}$  in the low ionic strength ( $\sim 8 \text{ mmol L}^{-1}$ ) groundwater systems varied widely. At pH 3.5 in the  $\text{HNO}_3$ -affected groundwater only 29%  $^{90}\text{Sr}$  was sorbed after 48 h. In the unbuffered (pH 5.5) and  $\text{HCO}_3^-$ -buffered (pH 7.2) groundwater the degree of  $^{90}\text{Sr}$  sorption increased significantly, to 61.8% and 98.9%, respectively, with the highest  $K_d$  ( $899 \pm 29 \text{ L kg}^{-1}$ ) observed in the buffered groundwater. Sorption of  $^{90}\text{Sr}$  in the pH 11 artificial Magnox tank liquor (ionic strength  $29.2 \text{ mmol L}^{-1}$ ) was lower ( $\sim 79\%$ ) than the buffered groundwater system at 48 h.

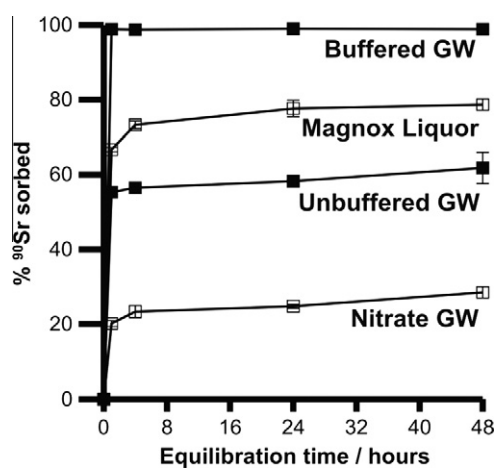


**Fig. 3.** Sorption kinetics of  $^{90}\text{Sr}$  uptake from experimental groundwater solutions onto aquifer sediments (solid:solution =  $100 \text{ g L}^{-1}$ ;  $[\text{Sr}] = 1 \text{ mg L}^{-1}$ ).

The pH dependence of  $^{90}\text{Sr}$  sorption to the sediment in the unbuffered groundwater solution (Table 1, Solution B) is given in Fig. 4a. At low pH, a low level of sorption ( $<10\%$ ) is observed, before a rapid increase in sorption between pH 4 and 6 (i.e. the sorption edge). Between pH 6 and 8, the pH commonly found within the Sellafield sub-surface (Sellafield Ltd., 2008), there is almost complete ( $>99\%$ ) sorption of  $^{90}\text{Sr}$  to the sediments. Above pH 8, the amount of  $\text{Sr}^{2+}$  sorbed decreased to  $92.6 \pm 1.3\%$  at pH 10. When the  $^{90}\text{Sr}$  sorption behaviour for synthetic groundwaters and Magnox liquor (see Table 2) is plotted in Fig. 4 it is possible to compare these data. In the groundwater systems the percentage of  $^{90}\text{Sr}$  sorbed correlates within error to the pH sorption edge data. However, the simulated Magnox liquor shows less sorption than would be expected for a groundwater based system at the same pH indicating that another effect influences Sr sorption behaviour in this system.

### 3.3. Cation competition effects with $\text{Na}^+$ and $\text{Ca}^{2+}$

Fig. 5 shows the effect of increasing concentrations of Na and Ca concentration in the  $\text{HCO}_3^-$ -buffered groundwater system on  $^{90}\text{Sr}$  sorption. Data for  $^{90}\text{Sr}$  sorption at 48 h in  $\text{HCO}_3^-$ -buffered groundwater and artificial Magnox liquor solutions have also been plotted as a function of their total ionic strength. Generally, the percentage of  $^{90}\text{Sr}$  sorbed decreased with increasing ionic strength, however this effect is most pronounced in solutions with total ionic strength greater than  $5 \text{ mmol L}^{-1}$ . In experiments with the highest ionic strength ( $0.1 \text{ mol L}^{-1}$ ),  $^{90}\text{Sr}$  sorption is  $41.4 \pm 1.9\%$  in the  $\text{Na}^+$  solution and  $21.3 \pm 2.7\%$  in the  $\text{Ca}^{2+}$  solution. The high level of sorption ( $>98\%$ ) observed in the  $\text{HCO}_3^-$ -buffered groundwater system ( $\text{IS} = 8 \text{ mmol L}^{-1}$ ), is consistent with the high sorption ( $>99\%$ ) observed in low ionic strength ( $\text{IS} = 4\text{--}10 \text{ mmol L}^{-1}$ ) Na and Ca solutions. Magnox liquor has a higher ionic strength

**Table 2**

Experimental pH and Sr-90 distribution coefficients determined after 48 h.

	Groundwater solution	Initial solution pH	pH at 48 h	<sup>90</sup> Sr sorption (% ±1σ)	K <sub>d</sub> (L kg <sup>-1</sup> ±1σ)
A	Nitric acid affected GW	3.5	3.97–3.99	28.5 ± 1.5	4 ± 0.3
B	Unbuffered GW	5.5	5.23–5.30	61.8 ± 4.2	16 ± 3
C	Bicarbonate buffered GW	7.2	7.01–7.19	98.9 ± 0.04	898 ± 29
D	Magnox tank liquor	11.0	7.78–7.90	78.9 ± 1.5	37 ± 3

**Table 3**Sr K-edge EXAFS model fitting parameters where *n* is the occupancy (±25%), *r* is the interatomic distance (±0.02 Å for the first shell, ±0.05 Å for outer shells), 2σ<sup>2</sup> is the Debye–Waller factor (±25%), and *R* is the least squares residual.

Sample	Shell	<i>n</i>	<i>R</i> (Å)	2σ <sup>2</sup> (Å <sup>2</sup> )	<i>R</i>
Buffered GW 10 days	O	9	2.61	0.022	30.7
Buffered GW 365 days	O	9.3	2.58	0.022	27.6
Magnox 10 days	O	8.5	2.59	0.021	27.9
Magnox 365 days	O	8.9	2.60	0.024	35.0
Sr <sup>2+</sup> solution	O	9.1	2.58	0.031	26.3

(29.2 mmol L<sup>-1</sup>) dominated by Na<sup>+</sup>. The % sorption is consistent with <sup>90</sup>Sr sorption in equivalent ionic strength Na<sup>+</sup> solution, indicating that ionic strength influences the extent of Sr sorption in this system. This ionic strength effect can also be seen in Langmuir isotherm fits for Sr sorption in HCO<sub>3</sub>-buffered groundwater and

Magnox tank liquor (Fig. 6). The calculated S<sub>max</sub> for Sr<sup>2+</sup> in the buffered groundwater (IS = 8 mmol L<sup>-1</sup>) was 32 ± 6 μmol g<sup>-1</sup> (R<sub>2</sub> = 0.82). Due to its 2+ charge, maximum Sr adsorption in this solution may, therefore, utilise 64 ± 12 μeq g<sup>-1</sup> (or ~80 ± 15%) of the total measured sediment CEC of 82 ± 52 μeq g<sup>-1</sup>. When the isotherm experiments were repeated using the Magnox liquor solution (IS = 29.2 mmol L<sup>-1</sup>), the calculated S<sub>max</sub> for Sr<sup>2+</sup> adsorption was just 2.2 ± 0.4 μmol g<sup>-1</sup> (R<sub>2</sub> = 0.89). In the higher ionic strength solution, therefore, only ~5 ± 1% of the total CEC is available for Sr<sup>2+</sup> adsorption.

### 3.4. Long-term sorption experiments and X-ray absorption spectroscopy

Data from sequential extractions (Fig. 7) indicates that in the buffered groundwater total <sup>90</sup>Sr sorption increased from around

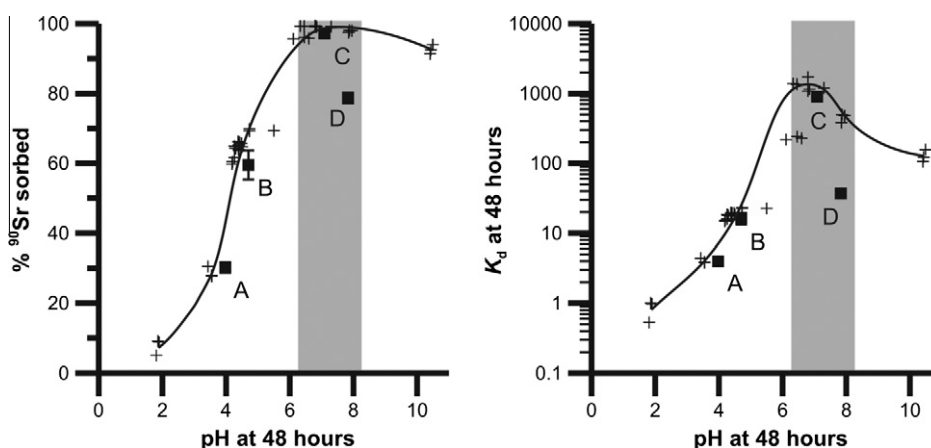


**Fig. 4.** Effect of variation in pH on <sup>90</sup>Sr sorption and K<sub>d</sub> (logarithmic scale). Data marked with (+) are from experiments in a sediment–water system based on Solution B in Table 1 (ionic strength = 5 mmol L<sup>-1</sup>; solid:solution = 100 g L<sup>-1</sup>; [Sr] = 1 mg L<sup>-1</sup>). Also plotted % <sup>90</sup>Sr sorption and K<sub>d</sub> calculated after 48 h for groundwater compositions in Table 2. (A) Nitric acid affected groundwater; (B) unbuffered groundwater; (C) buffered groundwater; (D) Magnox tank liquor. Grey shaded area outlines the pH range measured at the Sellafeld nuclear site (Sellafeld Ltd., 2008).

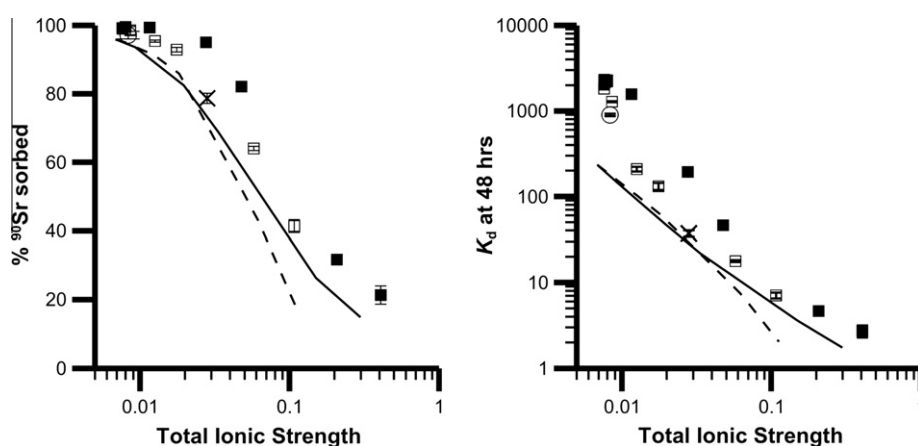


**Fig. 5.** Effect of increasing Na<sup>+</sup> (□) and Ca<sup>2+</sup> (■) concentration in a groundwater based sediment–water system on <sup>90</sup>Sr Sorption. Also plotted % <sup>90</sup>Sr sorption calculated after 48 h for buffered groundwater (○) and Magnox tank liquor (×) versus their total cation concentration (ionic strength, mol L<sup>-1</sup>). Solid and dashed lines represent results from PHREEQC cation exchange modelling considering the effects of Ca<sup>2+</sup> and Na<sup>+</sup> concentrations respectively.

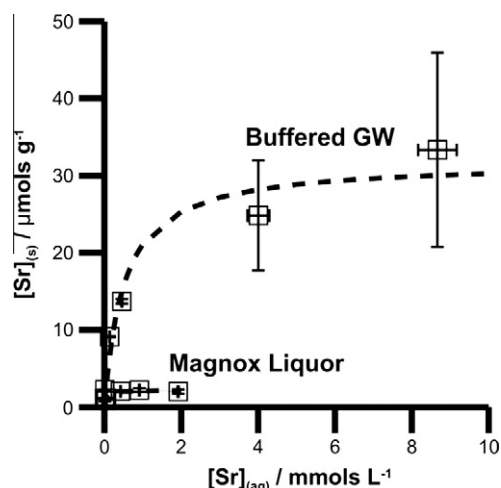


**Fig. 6.**  $^{90}\text{Sr}$  sorption isotherms calculated for bicarbonate buffered groundwater ("Buffered GW") and simulated Magnox tank liquor ("Magnox Liquor") sediment-waters after 48 h equilibration. Experimental data ( $\square$ ) have been fitted to modelled Langmuir isotherms (dashed line) ( $R_2 = 0.83$  and  $0.93$ , respectively).

60% at 10 days to around 80% at 365 days. Total  $^{90}\text{Sr}$  sorption in the Magnox systems, however, was between 60% and 70% at all time points. In both systems the majority (70–85%) of the solid associated  $^{90}\text{Sr}$  was  $\text{MgCl}_2$  exchangeable, even after 365 days. Only a small fraction (5–10%) of  $^{90}\text{Sr}$  was found to be present in the weak acid extractable phase in both systems, and even less (1–3%) in the hydroxylammonium chloride reducible phase. The amount of  $^{90}\text{Sr}$  that is residual (not extracted) was  $7 \pm 1\%$  after 365 days in the buffered groundwater, and  $4 \pm 1\%$  in the Magnox liquor experiments respectively. EXAFS spectra (Fig. 8) collected from all samples at 10 and 365 days could be fitted with a single shell of 8.5–9.3 O backscatters at 2.58–2.61 Å (as could the  $\text{Sr}^{2+}$  solution data). Additional shells of backscatters at distances beyond 3 Å were not justified as there were no additional peaks present in Fourier transforms and no significant improvement in  $R$  could be achieved. There was also no change in EXAFS spectra between samples taken at 10 and 365 days.

#### 4. Discussion

##### 4.1. pH 2–10 adsorption behaviour

The  $\text{HNO}_3$ -affected groundwater, unbuffered groundwater and  $\text{HCO}_3^-$ -buffered groundwater systems had pHs of  $\sim 3.5$ ,  $\sim 5.5$  and  $\sim 7.2$ , respectively. In this range of low ionic strength systems ( $< 10 \text{ mmol L}^{-1}$ ), variation in pH was the main influence on  $^{90}\text{Sr}$  sorption behaviour. Very little  $^{90}\text{Sr}$  is expected to be sorbed below

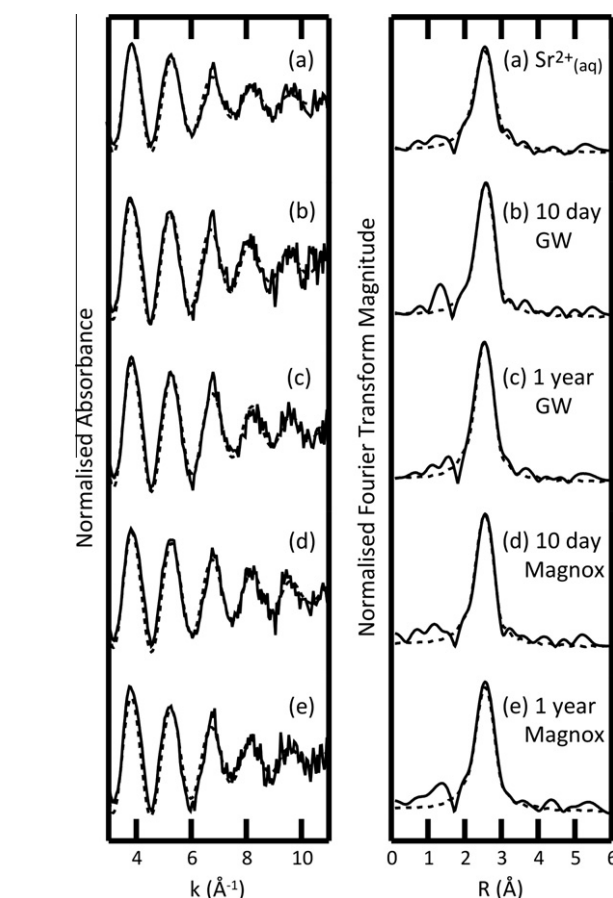


**Fig. 8.** Background subtracted Sr K-edge EXAFS spectra (left hand side) and related Fourier transformations (right hand side) collected from a  $3000 \text{ mg L}^{-1} \text{ Sr}^{2+}$  solution and sediment samples aged with  $\text{Sr}^{2+}$  for 10 or 365 days in buffered groundwater ("GW") or artificial Magnox tank liquor ("Magnox"). Dashed lines represent model fits produced in DLExcurv V1.0 using the parameters listed in Table 3.

pH 4 due to the protonation of specific sorption sites on mineral surfaces which would prevent the electrostatic (outer-sphere) adsorption of Sr (Krauskopf and Bird, 1995; Kulczycki et al., 2002); however in the experiments  $\sim 30\%$   $^{90}\text{Sr}$  sorbed to the sediment at pH 4 and  $\sim 10\%$  sorbed at pH 2. The permanent structural negative charges present in clay minerals may account for this sorption observed at low pH (Coppin et al., 2002) and has been observed in previous experiments where Sr was adsorbed to pure clay minerals at low pH (Parkman et al., 1998; Chen and Hayes, 1999). In addition, it has been shown that in low pH conditions organic matter can act as a sorbing phase for metal ions in solution

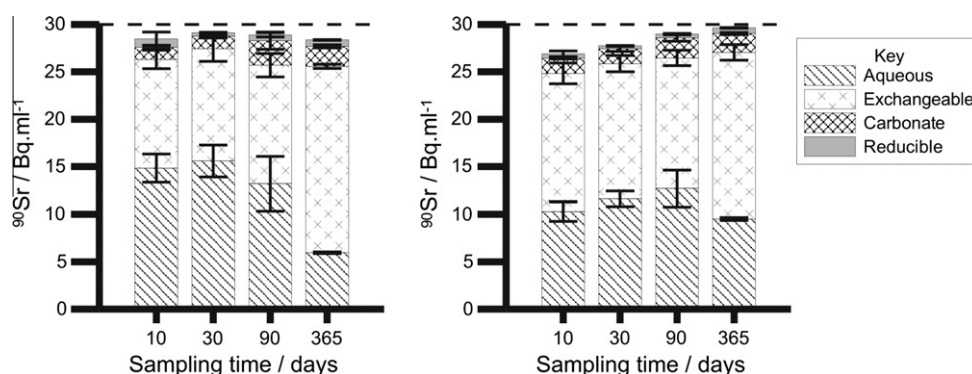


**Fig. 7.**  $^{90}\text{Sr}$  concentrations recovered in sequential extraction leachates from sediments aged in bicarbonate buffered groundwater solution (left hand side) or artificial Magnox tank liquor (right hand side). Dashed line at  $30 \text{ Bq mL}^{-1}$  equates to 100% recovery.

(Small et al., 1999; Langley et al., 2009) and thus may also contribute to the  $^{90}\text{Sr}$  sorption observed at very low pH in these experiments. The sorption edge for Sr onto the sediment was observed in the pH 4–6 range, consistent with the PZC for chlorite, the dominant clay mineral present within the sediments ( $\text{PZC}_{\text{chlorite}} = 4.7$ , Alvarez-Silva et al., 2010). Illite is present as a minor clay fraction in the sediments and has a lower PZC than chlorite ( $\text{PZC}_{\text{illite}} = 2.5$ , Hussain et al., 1996; Zhuang and Yu, 2002), which may also explain why some sorption of  $^{90}\text{Sr}$  was seen at low pH.

Between pH 6 and 8 is a zone of very high sorption, where the maximum  $K_d$  of  $\sim 10^3 \text{ L kg}^{-1}$  occurs at around pH 7. This is the pH range most commonly found in groundwaters at the UK Sellafield site (Sellafield Ltd., 2008). The high adsorption observed in this pH region is consistent with the sorption maximum observed for Sr (and other  $\text{M}^{2+}$  ions) on clay materials (Syed Hakimi Sakuma Syed, 1995; Lu and Mason, 2001; Solecki, 2006). At alkaline pH, although  $^{90}\text{Sr}$  sorption remains generally high there is a drop in sorption at around pH 10 with an order of magnitude decrease in  $K_d$  to  $\sim 10^2 \text{ L kg}^{-1}$ . This is attributed to the addition of NaOH to fix the pH, increasing the total ionic strength present ( $\sim 20 \text{ mmol L}^{-1}$ ) to a level sufficient for cation exchange to occur, therefore, inhibiting  $^{90}\text{Sr}$  sorption.

#### 4.2. Effect of ionic strength

Cation competition effects are not observed to be important in low ionic strength systems, such as the  $\text{HCO}_3^-$ -buffered groundwater ( $\text{IS} = 8 \text{ mmol L}^{-1}$ ) and solutions containing low concentrations (up to  $5 \text{ mmol L}^{-1}$ ) of  $\text{Ca}^{2+}$  and/or  $\text{Na}^+$ . At higher ionic strengths, particularly those relevant to contaminated liquors found at nuclear sites, competing ions cause a reduction in  $^{90}\text{Sr}$  sorption (Zachara et al., 2004; Hull and Schafer, 2008). In the Magnox tank liquor system ( $\text{IS} = 29 \text{ mmol L}^{-1}$ ),  $^{90}\text{Sr}$  sorption was less than low ionic strength solutions at the same pH (Fig. 4), and calculated  $K_d$  values are reduced by nearly two orders of magnitude from  $\sim 10^3$  to  $\sim 10^1 \text{ L kg}^{-1}$ . Thus, it is apparent that increasing ionic strength from 8 to  $29 \text{ mmol L}^{-1}$  and beyond has a major impact on Sr sorption. Further evidence for this is shown in the isotherm data for both the buffered and the Magnox systems. There is a large difference in the observed  $S_{\text{max}}$  ( $32 \pm 6 \mu\text{mol g}^{-1}$  for buffered groundwater versus  $2.2 \pm 0.4 \mu\text{mol g}^{-1}$  for Magnox liquor). The  $S_{\text{max}}$  for the buffered system implies that the sediment CEC is only around 20% saturated by the background electrolyte in this system, and therefore a large exchange capacity remains available for  $\text{Sr}^{2+}$  adsorption. In experiments using the Magnox tank liquor, however, the  $S_{\text{max}}$  is markedly lower, implying that around 95% of the CEC is saturated by the background electrolyte prior to Sr addition.

Fig. 5 shows a PHREEQC ion exchange model fit to the experimental  $^{90}\text{Sr}$  sorption data as a function of increasing ionic strength ( $\text{CaCl}_2$  and  $\text{NaCl}$  addition experiments). The model fits shown were produced after varying the exchange site concentration (CEC) and the generic exchange constants (Appelo and Postma, 2005), to best fit the experimental data, as shown below:

$$\text{CEC} = 3 \times 10^{-2} \text{ mol L}^{-1}$$



The ion exchange model closely follows the experimental data suggesting that around 90–95% of the observed  $^{90}\text{Sr}$  sorption is accounted for by ion exchange processes. However, despite varying the exchange constants and increasing the CEC to around four

times the measured value, the model cannot fully explain the measured  $^{90}\text{Sr}$  sorption, or the very high  $K_d$  values observed at low ionic strengths. This implies that an additional sorption site that is highly adsorbing with respect to Sr is present in the sediments. This enhanced sorption behaviour was not observed in similar previous studies that used sediments with generally much lower organic matter content ( $<0.1\%$  versus  $0.56\%$ ) (Small et al., 2000; Randall, 2008). It is, therefore, tentatively suggested that the higher total adsorption observed in this study is due to enhanced  $\text{Sr}^{2+}$  sorption to organic matter that is not captured within the cation exchange model.

#### 4.3. Sr-sorption in long-term experiments

Strontium sorption in long-term experiments for both  $\text{HCO}_3^-$ -buffered groundwater and Magnox liquor was lower than that observed in the pH titration or ionic strength experiments (around 50% and 65% respectively after 10 days incubation), however, this is attributed to the much lower solid:solution ratio used in these experiments ( $20 \text{ g L}^{-1}$  versus  $100 \text{ g L}^{-1}$ ), plus the higher concentration of  $\text{Sr}^{2+}$  ( $20 \text{ mg L}^{-1}$  versus  $1 \text{ mg L}^{-1}$ ). Over the course of a year, however, total sorption increased in both experimental solutions, to around 80% and 70%, respectively. This slow increase in adsorption is most likely due to interparticle diffusion of  $^{90}\text{Sr}$  into aggregates and clay particles over time. The sequential extractions performed on all samples found that more than 70% of sediment-associated  $^{90}\text{Sr}$  was exchangeable with  $\text{MgCl}_2$ , indicating that weak outer-sphere adsorption is the predominant mechanism for Sr sorption in both groundwaters and Magnox leak fluids. The percentage of Sr found to be associated with carbonate and reducible phases was less than 5% in all samples, and there was no increase or decrease in the proportion of Sr in the weak acid extraction phase over a year. This indicates that carbonates or reducible phases are not significant sorbing phases in the simulant systems. Further evidence for the mechanism of Sr sorption is offered by modelled EXAFS data. Strontium K-edge EXAFS spectra collected from sediments incubated with  $\text{HCO}_3^-$ -buffered groundwater reveal  $\sim 9$  Sr–O bond distances at  $\sim 2.60 \text{ \AA}$ , with no other features, indicating that Sr sorption is outer-sphere in a pH controlled system. The same Sr–O bond distances at  $\sim 2.60 \text{ \AA}$  are found in Sr K-edge EXAFS spectra collected from sediments incubated in Magnox liquor, also indicating that outer sphere sorption predominates. There is no change in the Sr coordination environment for both samples that were incubated for 365 days, indicating that Sr adsorption remains outer sphere in nature. This result is consistent with the sequential extraction results from parallel samples above.

### 5. Conclusions and Implications for $^{90}\text{Sr}$ mobility

Strontium-90 mobility at contaminated nuclear sites will be affected by the pH, ionic strength and chemical composition of groundwaters and leak fluids. The results of this study support previous findings by Small et al. (2000) suggesting the adsorption of Sr to west Cumbrian sediments at neutral pH can, to a first order approximation, be modelled as a cation exchange process. Fig. 9 outlines a conceptual model for  $^{90}\text{Sr}$  sorption in a range of groundwater compositions expected at UK nuclear sites. Overall, optimal retardation of Sr migration occurs when the pH is between 6 and 8 and ionic strength is lower than  $0.01 \text{ mol L}^{-1}$ , which is typical of groundwaters in the west Cumbria area (Wilkins et al., 2007). Under these conditions Sr is bound to sediments as outer sphere complexes.

Magnox tank liquors are at a higher pH than groundwaters measured at Sellafield, but buffering reactions with sediments can rapidly reduce pH to circumneutral values.  $K_d$  values found for Magnox liquor are nearly two orders of magnitude less than

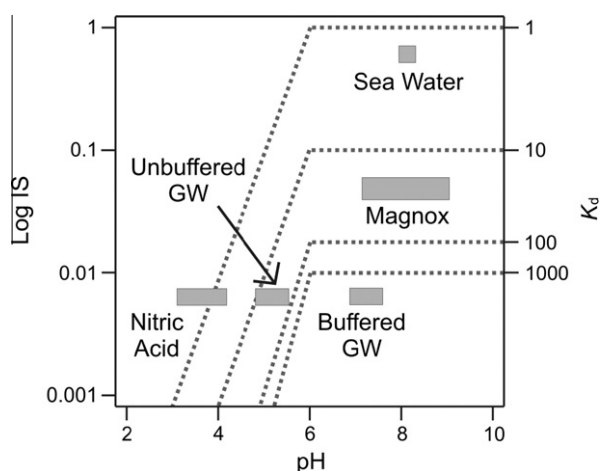


**Fig. 9.** Conceptual model of the variation in  $^{90}\text{Sr}$   $K_d$  expected in contaminated groundwaters equilibrated with Sellafield sediments (IS = ion strength in  $\text{mol L}^{-1}$ ;  $K_d$  = Sr distribution coefficient in  $\text{L kg}^{-1}$ ).

for buffered groundwater solutions. It is, therefore, concluded that the higher ionic strength caused by the presence of competing ions, primarily  $\text{Na}^+$ , in the tank fluid results in the much lower sorption observed. Consideration of ionic strength effects may help to explain why significant migration of  $^{90}\text{Sr}$  has been observed at Sellafield where the *in situ* pH is in fact favourable for sorption. The apparent retardation factor (Rf) for  $^{90}\text{Sr}$  compared with  $^3\text{H}$  at Sellafield (rate of  $^3\text{H}$  migration,  $196 \text{ m a}^{-1}$  divided by rate of  $^{90}\text{Sr}$  migration,  $3.8 \text{ m a}^{-1}$ ) is approximately 52 (Vickery et al., 2005). As  $\text{Rf} = K_d + 1$ , therefore, it is possible to directly compare the experimental  $K_d$  calculated for artificial Magnox tank liquor ( $37 \text{ L kg}^{-1}$ ) in the sediments studied here with the observed field Rf. Both values are of similar magnitude, suggesting that the higher ionic strength of tank leak fluids may be a contributing factor in controlling the sorption behaviour of  $^{90}\text{Sr}$  at Sellafield. Furthermore, acidic and high  $\text{NO}_3^-$ -containing sources (McBeth et al., 2007; Law et al., 2010) have low pH and high ionic strength and under these conditions low  $^{90}\text{Sr}$  sorption may also be expected.

Finally, EXAFS data from this study shows that adsorbed Sr remains in weakly bound outer sphere surface complexes even after incubation for one year. This has clear implications with respect to scenarios where future sea level rise may result in seawater inundation of coastal sites. This would result in increased ionic strength in groundwaters, and, therefore, remobilisation of adsorbed  $^{90}\text{Sr}$  by cation exchange. However, this understanding could also be used in remediation strategies for contaminated sites. For example, soil washing techniques using high ionic strength fluids could be used to efficiently remove adsorbed  $^{90}\text{Sr}$  from sediments.

## Acknowledgements

The authors would like to thank Lesley Neve (University of Leeds) for help with XRD analysis of sediments and Gareth Law (University of Manchester) for sharing results of previous sediment characterisation work. Generic data on Magnox sludge liquor composition was kindly supplied in commercial confidence by Sellafield Ltd. via James Graham (National Nuclear Laboratory Ltd.). Linda Forbes (University of Leeds) is thanked for ICP-OES analysis. We also acknowledge support for synchrotron time at the ESRF and assistance from Sergey Nikitenko and Miguel Silveira during XAS data acquisition. This work was funded by an EPSRC industrial CASE doctoral training award to S.H.W., administered by National Nuclear Laboratory Ltd., and the UK Nuclear Decommissioning Authority. We also acknowledge support from NERC Grant NE/H007768/1.

## References

- Alvarez-Silva, M., Uribe-Salas, A., Mirnezami, M., Finch, J.A., 2010. The point of zero charge of phyllosilicate minerals using the Mular-Roberts titration technique. *Miner. Eng.* 23, 383–389.
- Appelo, C.A.J., Postma, D., 2005. *Geochemistry, Groundwater and Pollution*. A.A. Balkema, Leiden, The Netherlands.
- ASTM, 2006. D4972-01: Standard Test Method for pH of Soils, Annual Book of ASTM Standards. American Society for Testing and Materials, pp. 963–965.
- Bascetin, E., Atun, G., 2006. Adsorption behavior of strontium on binary mineral mixtures of Montmorillonite and Kaolinite. *Appl. Radiat. Isot.* 64, 957–964.
- Bilgin, B., Atun, G., Keceli, G., 2001. Adsorption of strontium on illite. *J. Radioanal. Nucl. Chem.* 250, 323–328.
- Binsted, N., 1998. EXCURV98: CLRC Daresbury Laboratory Computer Program, CLRC Daresbury, Warrington, UK.
- Binsted, N., Strange, R.W., Hasnain, S.S., 1993. Constrained and restrained refinement in EXAFS data-analysis with curved wave theory. *Japan. J. Appl. Phys. Part 1 – Regular Papers Short Notes & Review Papers* 32, 141–143.
- Burke, I.T., Livens, F.R., Lloyd, J.R., Brown, A.P., Law, G.W., McBeth, J.M., Ellis, B.L., Lawson, R.S., Morris, K., 2010. The fate of technetium in reduced estuarine sediments: combining direct and indirect analyses. *Appl. Geochem.* 25, 233–241.
- Chen, C.C., Hayes, K.F., 1999. X-ray absorption spectroscopy investigation of aqueous Co(II) and Sr(II) sorption at clay–water interfaces. *Geochim. Cosmochim. Acta* 63, 3205–3215.
- Choi, S., O'Day, P.A., Rivera, N.A., Mueller, K.T., Vairavamurthy, M.A., Seraphin, S., Chorover, J., 2006. Strontium speciation during reaction of kaolinite with simulated tank-waste leachate: bulk and microfocused EXAFS analysis. *Environ. Sci. Technol.* 40, 2608–2614.
- Chorover, J., Choi, S., Rotenberg, P., Serne, R.J., Rivera, N., Strepka, C., Thompson, A., Mueller, K.T., O'Day, P.A., 2008. Silicon control of strontium and cesium partitioning in hydroxide-weathered sediments. *Geochim. Cosmochim. Acta* 72, 2024–2047.
- Coppin, F., Berger, G., Bauer, A., Castet, S., Loubet, M., 2002. Sorption of lanthanides on smectite and kaolinite. *Chem. Geol.* 182, 57–68.
- Dyer, A., Chow, J.K.K., Umar, I.M., 2000. The uptake of caesium and strontium radioisotopes onto clays. *J. Mater. Chem.* 10, 2734–2740.
- Dzombak, D.A., Morel, F.M.M., 1990. *Surface Complexation Modelling: Hydroxyl Ferric Oxides*. John Wiley and Sons, New York.
- Gray, J., Jones, S.R., Smith, A.D., 1995. Discharges to the environment from the Sellafield site, 1951–1992. *J. Radiol. Prot.* 15, 99–131.
- Gu, B.H., Wu, W.M., Ginder-Vogel, M.A., Yan, H., Fields, M.W., Zhou, J., Fendorf, S., Criddle, C.S., Jardine, P.M., 2005. Bioreduction of uranium in a contaminated soil column. *Environ. Sci. Technol.* 39, 4841–4847.
- Gurman, S.J., Binsted, N., Ross, I., 1984. A rapid, exact curved-wave theory for EXAFS calculations. *J. Phys. C – Solid State Phys.* 17, 143–151.
- Higgo, J.J.W., 1987. Clay as a barrier to radionuclide migration. *Prog. Nucl. Energy* 19, 173–207.
- Honty, M., De Craen, M., Wang, L., Madejová, J., Czimerová, A., Pentrák, M., Stríček, I., Van Geet, M., 2010. The effect of high pH alkaline solutions on the mineral stability of the Boom clay – batch experiments at 60 °C. *Appl. Geochem.* 25, 825–840.
- Hull, L.C., Schafer, A.L., 2008. Accelerated transport of Sr-90 following a release of high ionic strength solution in vadose zone sediments. *J. Contam. Hydrol.* 97, 135–157.
- Hussain, S.A., Demirci, S., Özbayoglu, G., 1996. Zeta potential measurements on three clays from Turkey and effects of clays on coal flotation. *J. Colloid Interface Sci.* 184, 535–541.
- Khan, S.A., Riaz ur, R., Khan, M.A., 1995. Sorption of strontium on bentonite. *Waste Manage.* 15, 641–650.
- Krauskopf, K.B., Bird, D.K., 1995. *Introduction to Geochemistry*. McGraw-Hill, New York.
- Kulczycki, E., Ferris, F.G., Fortin, D., 2002. Impact of cell wall structure on the behavior of bacterial cells as sorbents of cadmium and lead. *Geomicrobiol. J.* 19, 553–565.
- Langley, S., Gault, A.G., Ibrahim, A., Takahashi, Y., Renaud, R., Fortin, D., Clark, I.D., Ferris, F.G., 2009. Sorption of strontium onto bacteriogenic iron oxides. *Environ. Sci. Technol.* 43, 1008–1014.
- Law, G.T.W., Geissler, A., Boothman, C., Burke, I.T., Livens, F.R., Lloyd, J.R., Morris, K., 2010. Role of nitrate in conditioning aquifer sediments for technetium bioreduction. *Environ. Sci. Technol.* 44, 150–155.
- Limousin, G., Gaudet, J.P., Charlet, L., Szenknect, S., Barthès, V., Krimissa, M., 2007. Sorption isotherms: a review on physical bases, modeling and measurement. *Appl. Geochem.* 22, 249–275.
- Liu, W.C., Lo, J.G., Tsai, C.M., 1991. Sorption of Cs, Sr and Co on andesite and coral limestone. *Radiochim. Acta* 52 (3), 169–175.
- Livens, F.R., Baxter, M.S., 1988. Chemical associations of artificial radionuclides in Cumbrian soils. *J. Environ. Radioact.* 7, 75–86.
- Lu, N.P., Mason, C.F.V., 2001. Sorption-desorption behavior of strontium-85 onto montmorillonite and silica colloids. *Appl. Geochem.* 16, 1653–1662.
- Marinini, D.V., Brown, G.N., 2000. Studies of sorbent/ion-exchange materials for the removal of radioactive strontium from liquid radioactive waste and high hardness groundwaters. *Waste Manage. (Oxford)* 20, 545–553.
- McBeth, J.M., Lear, G., Lloyd, J.R., Livens, F.R., Morris, K., Burke, I.T., 2007. Technetium reduction and reoxidation in aquifer sediments. *Geomicrobiol. J.* 24, 189–197.

- McMillan, A.A., Heathcote, J.A., Klinck, B.A., Shepley, M.G., Jackson, C.P., Degnan, P.J., 2000. Hydrogeological characterization of the onshore quaternary sediments at Sellafield using the concept of domains. *Q. J. Eng. Geol. Hydrogeol.* 33, 301–323.
- Nikitenko, S., Beale, A.M., van der Eerden, A.M.J., Jacques, S.D.M., Leynaud, O., O'Brien, M.G., Detollenaere, D., Kaptein, R., Weckhuysen, B.M., Bras, W., 2008. Implementation of a combined SAXS/WAXS/QEXAFS set-up for time-resolved in situ experiments. *J. Synchrotron Radiat.* 15, 632–640.
- O'Day, P.A., Newville, M., Neuhoff, P.S., Sahai, N., Carroll, S.A., 2000. X-ray absorption spectroscopy of strontium(II) coordination: I. Static and thermal disorder in crystalline, hydrated, and precipitated solids and in aqueous solution. *J. Colloid Interface Sci.* 222, 184–197.
- O'Hara, M.J., Burge, S.R., Grate, J.W., 2009. Automated radioanalytical system for the determination of Sr-90 in environmental water samples by Y-90 Cherenkov radiation counting. *Anal. Chem.* 81, 1228–1237.
- Parkhurst, D.L., Appelo, C.A.J., 1999. User's guide to PHREEQC (version 2) – a computer program for speciation, batch-reaction, one-dimensional transport, and inverse geochemical calculations. US Geol. Surv. Water Resour. Invest. Rep. 99-4259.
- Parkman, R.H., Charnock, J.M., Livens, F.R., Vaughan, D.J., 1998. A study of the interaction of strontium ions in aqueous solution with the surfaces of calcite and kaolinite. *Geochim. Cosmochim. Acta* 62, 1481–1492.
- Patterson, R.J., Spoel, T., 1981. Laboratory measurements of the strontium distribution coefficient  $K_{dsr}$  for sediments from a shallow sand aquifer. *Water Resour. Res.* 17, 513–520.
- Pors Nielsen, S., 2004. The biological role of strontium. *Bone* 35, 583–588.
- Randall, M.G., 2008. LLWR Lifetime Project: Sorption Parameters for the LLWR Geosphere. Report Number (08) 9451, Nexia Solutions for and On Behalf of the Low Level Waste Repository Site Licence Company. <<http://www.llwrsite.com/environmental-safety-case/esc-documentation/level-3>> (accessed September 2011).
- Ravel, B., Newville, M., 2005. ATHENA, ARTEMIS, HEPHAESTUS: data analysis for X-ray absorption spectroscopy using IFEFFIT. *J. Synchrotron Radiat.* 12, 537–541.
- Sahai, N., Carroll, S.A., Roberts, S., O'Day, P.A., 2000. X-ray absorption spectroscopy of strontium(II) coordination: II. Sorption and precipitation at kaolinite, amorphous silica, and goethite surfaces. *J. Colloid Interface Sci.* 222, 198–212.
- Saunders, J.A., Toran, L.E., 1995. Modeling of radionuclide and heavy metal sorption around low- and high-pH waste disposal sites at Oak Ridge, Tennessee. *Appl. Geochem.* 10, 673–684.
- Schramm, E., Scripture, E.W., 1925. The particle analysis of clays by sedimentation 1. *J. Am. Ceram. Soc.* 8, 243–252.
- Sellafield Ltd., 2008. Land Quality Programme Groundwater Monitoring Annual Report, Sellafield Ltd. <[http://www.sellafielddata.com/land/pages/groundwater\\_monitoring.html](http://www.sellafielddata.com/land/pages/groundwater_monitoring.html)> (accessed September 2009).
- Sellafield Ltd., 2009. Generic Basis for Inventory Challenge – Legacy Alkaline Sludge Systems, Sellafield Ltd., Cumbria, UK.
- Small, T.D., Warren, L.A., Roden, E.E., Ferris, F.G., 1999. Sorption of strontium by bacteria, Fe(III) oxide, and bacteria-Fe(III) oxide composites. *Environ. Sci. Technol.* 33, 4465–4470.
- Small, J.S., Randall, M.G., Abratis, P.K., Humphreys, P.N., 2000. Modelling the ion exchange properties of geological materials and implications for radionuclide mobility. In: Greig, J.A. (Ed.), *Ion Exchange at the Millennium: Proc. IEX 2000*. Published On Behalf of SCI by Imperial College Press, London, UK, pp. 124–132.
- Solecki, J., 2006. Investigation of Sr-85 adsorption in the presence of Na<sup>+</sup>, K<sup>+</sup> and Cs<sup>+</sup> on selected soils from different horizons. *J. Radioanal. Nucl. Chem.* 268, 357–364.
- Sposito, G., 1989. *The Chemistry of Soils*. Oxford University Press, New York, Oxford.
- Standing, W.J.F., Oughton, D.H., Salbu, B., 2002. Potential remobilization of Cs-137, Co-60, Tc-99 and Sr-90 from contaminated Mayak sediments river and estuary environments. *Environ. Sci. Technol.* 36, 2330–2337.
- Strand, P., Brown, J.E., Drozhko, E., Mokrov, Y., Salbu, B., Oughton, D., Christensen, G.C., Amundsen, I., 1999. Biogeochemical behaviour of Cs-137, and Sr-90 in the artificial reservoirs of Mayak PA, Russia. *Sci. Total Environ.* 241, 107–116.
- Syed Hakimi Sakuma Syed, A., 1995. Competitive adsorption of <sup>90</sup>Sr on soil sediments, pure clay phases and feldspar minerals. *Appl. Radiat. Isot.* 46, 287–292.
- Tenderholt, A., Hedman, B., Hodgson, K.O., 2007. PySpline: a modern, cross-platform program for the processing of raw averaged XAS edge and EXAFS data. In: Hedman, B.P.P. (Ed.), *X-Ray Absorption Fine Structure-XAFS13*. Aip Conf. Proc., pp. 105–107.
- Tessier, A., Campbell, P.G.C., Bisson, M., 1979. Sequential extraction procedure for the speciation of particulate trace-metals. *Anal. Chem.* 51, 844–851.
- Thompson, A., Steefel, C.I., Perdrial, N., Chorover, J., 2010. Contaminant desorption during long-term leaching of hydroxide-weathered Hanford sediments. *Environ. Sci. Technol.* 44, 1992–1997.
- Thorpe, C.L., Lloyd, J.R., Law, G.T.W., Burke, I.T., Shaw, S., Bryan, N.D., Morris, K., 2012. Strontium sorption and precipitation behaviour during bioreduction in nitrate impacted sediments. *Chem. Geol.* 306–307, 114–122.
- Tomic, S., Searle, B.G., Wander, A., Harrison, N.M., Dent, A.J., Mosselmans, J.F.W., Inglesfield, J.E., 2005. New Tools for the Analysis of EXAFS: The DL\_EXCURV Package. CCLRC Technical Report DL-TR-2005-00, ISSN: 1362-0207, Daresbury SRS 2005.
- Torstenfeld, B., Andersson, K., Allard, B., 1982. Sorption of strontium and cesium on rocks and minerals. *Chem. Geol.* 36, 123–137.
- Trivedi, P., Axe, L., 1999. A comparison of strontium sorption to hydrous aluminum, iron, and manganese oxides. *J. Colloid Interface Sci.* 218, 554–563.
- Vickery, A.C., Coleman, I.A., Glaister, C.G., 2005. A Practicable and Integrated Groundwater Monitoring Programme Proposed for the Sellafield Site. Report 050268/02, Westlakes Scientific Consulting Ltd. <[http://www.sellafielddata.com/land/pages/groundwater\\_monitoring.html](http://www.sellafielddata.com/land/pages/groundwater_monitoring.html)> (accessed September 2011).
- Whittig, L.D., Allardice, W.R., 1986. X-ray diffraction techniques. In: Klute, A. (Ed.), *Methods of Soil Analysis Part 1: Physical and Mineralogical Methods* American Society of Agronomy, Madison, Wisconsin.
- Wilkins, M.J., Livens, F.R., Vaughan, D.J., Beadle, I., Lloyd, J.R., 2007. The influence of microbial redox cycling on radionuclide mobility in the subsurface at a low-level radioactive waste storage site. *Geobiology* 5, 293–301.
- Zachara, J.M., Ainsworth, C.C., Brown, G.E., Catalano, J.G., McKinley, J.P., Qafoku, O., Smith, S.C., Szecsody, J.E., Traina, S.J., Warner, J.A., 2004. Chromium speciation and mobility in a high level nuclear waste vadose zone plume. *Geochim. Cosmochim. Acta* 68, 13–30.
- Zhuang, J., Yu, G.-R., 2002. Effects of surface coatings on electrochemical properties and contaminant sorption of clay minerals. *Chemosphere* 49, 619–628.